Computational Studies of the Energetics and Reaction Pathways of Molecular Transformations of Benzoheterocycles on Triosmium Clusters

Djamaladdin G. Musaev,* Taraneh Nowroozi-Isfahani, and Keiji Morokuma*

Emerson Center for Scientific Computation and Department of Chemistry, 1515 Dickey Drive, Emory University, Atlanta, Georgia 30322

Edward Rosenberg*

Department of Chemistry, University of Montana, Missoula, Montana 59812

Received August 17, 2005

Density functional theory (DFT) calculations have been performed on the series of complexes $Os_3(CO)_{10-n}(\mu_m\text{-}\eta^2\text{-(L-H)})(\mu\text{-H})$ (L = benzoxazole (**1**), benzothiazole (**2**), quinoline (**3**), indoline (**4**), 1,2,3,4-tetrahydroquinoline (**5**); for **1**−**5**, $n = 0$; $m = 2$; for **1′**−**3′**, $n = 1$, $m = 3$) and on the precursors to these complexes, $Os_3(CO)_{10}(CH_3CN)_2$ and $Os_3(CO)_{12}$. The optimized geometry of the coordinately unsaturated 44e system $Os_3(CO)_{10}$ is used as a reference point for evaluating the relative binding energies of the heterocycles and the acetonitrile and carbonyl ligands. A discussion of how the intramolecular trans/cis isomerization of $Os_3(CO)_{10}(CH_3CN)_2$ relates to the reactivity of this complex with the heterocyclic ligand is presented. The relative binding energies of the benzoheterocycles provide insight into the relative stability of the intermediates involved in the subsequent formation of the μ_3-nonacarbonyl derivatives $Os_3(CO)_9(\mu_3\text{-}\eta^2\text{-(L-2H)})(\mu\text{-H})_2$ (L = indoline (**4′**), 1,2,3,4-tetrahydroquinoline (**5′**)) from their μ-decacarbonyl precursors (**4** and **5**). The transition states for the N−H bond activation/decarbonylation that constitutes the transformation of **4** into **4′** have also been investigated. A discussion of the atomic and ligand group natural charges based on natural population analysis (NPA) calculations is presented as it relates to the donor abilities of the heterocycles and the polarization of the carbonyl ligands for the various structural types.

Introduction

Trimetallic clusters have been the focus of numerous studies relating to their usefulness as models for heterogeneous catalysts[1] and their use as homogeneous catalysts and as catalyst precursors.[2,3] In the particular case of triosmium clusters their chemistry is especially rich, owing to the stability of the trimetallic framework and to the availability of the "lightly stabilized" cluster $Os_3(CO)_{10}(CH_3CN)_2$, which reacts with a wide range of organic substrates at or slightly above room temperature to give 1:1 adducts in high yield.[2−4] This has in turn allowed detailed studies of the molecular transformations on the trimetallic framework, which have yielded valuable insights into the general mechanisms of the reactions of organic molecules on polymetallic surfaces. An example of this comes from the rich chemistry of bicyclic nitrogen heterocycles with $Os_3(CO)_{10}(CH_3CN)_2$, where the resulting complexes $Os_3(CO)_{10-n}(\mu_m\text{-(L−H)})(\mu\text{-H})$ (L = benzoxazole (**1**), benzothiazole (**2**), quinoline (**3**), indoline (**4**), 1,2,3,4-tetrahydroquinoline (**5**); for **1**−**5**, $n = 0$; $m = 2$; for **1′**−**3′**, $n = 1$, $m = 3$; Chart 1) and $Os_3(CO)_9(\mu_3\text{-(L-2H)})(\mu\text{-H})_2$ (L = indoline (**4′**), 1,2,3,4-tetrahydroquinoline (**5′**); Chart 1) and their subsequent thermal rearrangements have provided rationalizations for the kinetic trends observed in heterogeneously catalyzed hydrodenitrification (HDN).[5−7]

Subsequent studies with a wide range of benzoheterocycles revealed that, depending on the bonding mode of the organic ligand to the trimetallic core, the reactivity of the complex toward nucleophiles and electron

(1) Albert, M. R.: Yates, J. T. *The Surface Chemist's Guide to Organometallic Chemistry*; American Chemical Society: Washington, DC, 1987.

(2) Shriver, D. F.; Kaesz, H. D.; Adams, R. D. *The Chemistry of Metal Cluster Chemistry*; VCH: New York, 1990.

(3) Adams, R. D.; Cotton, F. A. *Catalysis by Di- and Polynuclear Metal Cluster Complexes*; Wiley-VCH: New York, 1998.

(4) Deeming, A. J. *Adv. Organomet. Chem.* **1986**, *26*, 1. For recent comprehensive reviews on ruthenium and osmium carbonyl cluster chemistry, see: (a) Deeming, A. J. In *Comprehensive Organometallic Chemistry II*; Abel, E. W., Stone, F. G. A., Wilkinson, G., Eds.; Pergamon: Oxford, U.K., 1995; Vol. 7, p 684. (b) Smith, A. K. In *Comprehensive Organometallic Chemistry II*; Abel, E. W., Stone, F. G. A., Wilkinson, G., Eds.; Pergamon: Oxford, U.K., 1995; Vol. 7, p 747. (c) Sappa, E. In *Comprehensive Organometallic Chemistry II*; Abel, E. W., Stone, F. G. A., Wilkinson, G., Eds.; Pergamon: Oxford, U.K., 1995; Vol. 7, p 804. (d) Pomeroy, R. K. In *Comprehensive Organometallic Chemistry II*; Abel, E. W., Stone, F. G. A., Wilkinson, G., Eds.; Pergamon: Oxford, U.K., 1995; Vol. 7, p 836. (e) Cifuentes, M. P.; Humphrey, M. G. In *Comprehensive Organometallic Chemistry II*; Abel, E. W., Stone, F. G. A., Wilkinson, G., Eds.; Pergamon: Oxford, U.K., 1995; Vol. 7, p 908.

(5) Fish, R. H.; Bianchini, C. In *Encyclopedia of Catalysis*; Horvath, I., Ed.; Wiley: New York, 2002; Vol. 3, p 564.

(6) Rosenberg, E.; Kolwaite, D. S.; Kabir, S. E.; Hardcastle, K. I.; McPhillips, T.; Duque, R.; Day, M. *Organometallics* **1996**, *15*, 1979.

(7) Rosenberg, E.; Arcia, E.; Kolwaite, D. S.; Hardcastle, K. I.; Ciurash, J.; Duque, R.; Gobetto, R.; Milone, L.; Osella, D.; Botta, M.; Dastrù, W.; Viale, A.; Fiedler. J. *Organometallics* **1998**, *17*, 415.

10.1021/om050711b CCC: $30.25
Publication on Web 10/20/2005

Chart 1. Structures of the Benzoheterocycle Complexes Based on Single-Crystal X-ray Structure Determinations and/or Multinuclear NMR Studies[a]

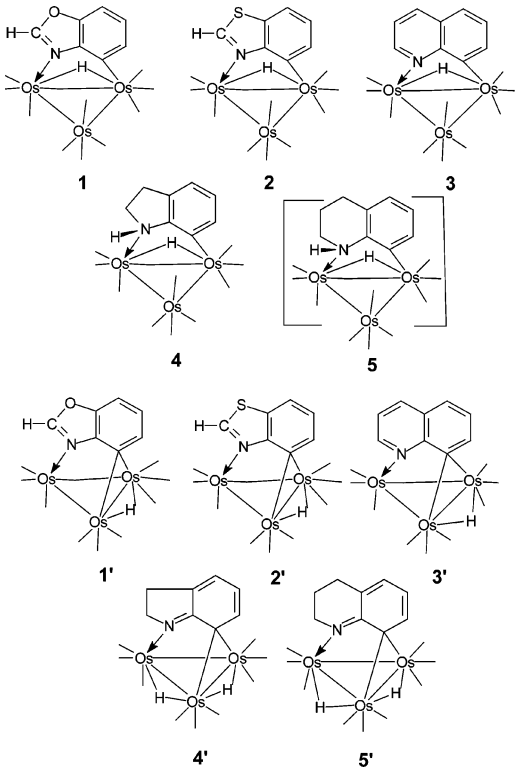

[a] Except for **5′**, which was not observed experimentally.

donors could be vastly different. In some cases binding of the heterocycle dramatically changed its reactivity relative to the free ligand.[8−10] Furthermore, the nature of the heterocycle had a significant impact on the thermal behavior and reactivity toward nucleophiles within the series of benzoheterocycle triosmium clusters.[11,12]

Despite these extensive experimental studies, there remain many questions related to the mechanisms of molecular transformations on the trimetallic framework, as well as the general mechanisms of the reactions of organic molecules on polymetallic surfaces that would benefit from comprehensive computational investigations. In fact, computational studies on understanding the rearrangements of ligands bound to trimetallic clusters,[13−18] their electronic structure,[8,19−21] and spectroscopic properties[8,22,23] have already yielded useful insights as to the origin of the reactivity trends in this class of compounds. However, to date there have been no computational studies that address the basic energetics of these systems and the factors governing their reaction pathways, partially because of the existence of technical difficulties. Recent developments in computational chemistry (the increase in computing power combined with the development of computational methods such as density functional and hybrid methods, including QM/MM and ONIOM) have made the use of quantum-mechanical studies accessible to chemists interested in gaining a deeper understanding of the structure and dynamics of trimetallic clusters. Here, we report our initial results of the density functional theory (DFT) calculations on the series of complexes mentioned above, along with a correlation and analysis of the data as they relate to previous experimental investigations.

Computational Procedures

Geometries and energetics of the proposed structures and transition states of the numerous intramolecular transformations in these species were calculated using the B3LYP density functional method[24] in conjunction with the standard LANL2DZ basis set of Hay and Wadt for Os atoms and 6-31(d) basis sets for the other elements.[25] The nature of all stationary points was confirmed by performing a normal-mode analysis. In addition, the nature of the calculated transition states was clarified using the pseudo-intrinsic reaction coordinates (IRC) approach.[26] Vibrational frequencies and the enthalpy (H) and Gibbs free energy (G) calculations of the systems were performed at 298.15 K and 1 atm pressure. The enthalpies and Gibbs free energies in solution were calculated from the gas-phase enthalpies or Gibbs free energies and the solvation free energies obtained from PCM calculations[27] with dichloromethane as the solvent. All calculations were performed without symmetry constraints utilizing the Gaussian03 program.[28] The chemically more interesting ΔH values will be used in the discussion, and corresponding ΔG values will be given in parentheses. Note that the difference between ΔG and ΔH surfaces reflects the entropy contribution to a given process or transformation.

Results and Discussion

The complexes **1**−**5**, studied in this paper, can be schematically considered as complexes of the heterocyclic ligand L (L = benzoxazole (**1**), benzothiazole (**2**),

(8) Nervi, C.; Gobetto, G.; Milone, L.; Viale, A.; Rokhsana, D.; Fiedler, J. Rosenberg, E. *Chem. Eur. J.* **2003**, *9*, 5749.
(9) Rosenberg, E.; Rokshsana, D.; Nervi, C. Gobetto, R.; Milone, L.; Viale, A.; Fiedler, J. *Organometallics* **2004**, *23*, 215.
(10) Abedin, J.; Bergman, B.; Holmquist, R.; Smith, R.; Rosenberg, E.; Ciurash, J.; Hardcastle, K. I.; Roe, J.; Vazquez, V.; Roe, C.; Kabir, S. E.; Roy, B.; Alam, S.; Azam, K. A. *Coord. Chem. Rev.* **1999**, *190−192*, 975.
(11) Bergman, B.; Holmquist, R. H.; Smith, R.; Rosenberg, E.; Hardcastle, K. I.; Visi, M.; Ciurash, J. *J. Am. Chem. Soc.* **1998**, *120*, 12818.
(12) Rosenberg, E.; Abedin, J.; Kabir, S. E.; Hardcastle, K. I. *Organometallics* **2004**, *23*, 3982.
(13) Kim, K. H.; Jung, J.; Han, Y. K. *Organometallics* **2004**, *23*, 3865.
(14) Bergamo, M.; Beringhelli, T.; D'Alphoso, G.; Garavaglia, L.; Mercandelli, P.; Moret, M.; Sironi, A. *J. Cluster Sci.* **2001**, *12*, 223.
(15) Khoroshun, D. V.; Inagaki, A.; Suzuki, H.; Vyboishchikov, S. F.; Musaev, D. G.; Morokuma, K. *J. Am. Chem. Soc.* **2003**, *125*, 9910.
(16) Riehl, J. F.; Koga, K.; Morokuma, K. *J. Am. Chem. Soc.* **1994**, *116*, 5414.
(17) Riehl, J. F.; Koga, K.; Morokuma, K. *J. Organometallics* **1994**, *13*, 4765.
(18) Riehl, J. F.; Koga, K.; Morokuma, K. *J. Organometallics* **1993**, *12*, 4788.
(19) Zimmerman, C.; Anson, C. E.; Eckerman, A. L.; Wunder, M.; Fischer, G.; Keihauer, I.; Herrling, E.; Pilawa, B.; Hampe, O.; Weigand, F.; Dehnen, S. *Inorg. Chem.* **2004**, *43*, 4595.
(20) Wadepohl, H.; Castano, M. E. *Chem. Eur. J.* **2003**, *9*, 5266.
(21) Morioka, T.; Ozawa, S.; Yamabe, T.; Masuda, H. *Polyhedron* **2003**, *22*, 3413.
(22) Wong, W. Y.; Choi, K. H.; Lin, Z. *Eur. J. Inorg. Chem.* **2002**, 2112.
(23) Kaupp, M. *Chem. Commun.* **1996**, 1141.
(24) (a) Becke, A. D. *J. Chem. Phys.* **1993**, *98,* 5648, (b) Becke, A. D. *Phys. Rev. A* **1988**, *38*, 3098. (c) Lee, C.; Yang, W.; Parr, R. G. *Phys. Rev. B* **1998**, *37,* 785.
(25) (a) Dunning, T. H., Jr. In *Modern Theoretical Chemistry*; Schaefer, H. F., III, Ed.; Plenum: New York, 1976; pp 1−28. (b) Hay, P. J.; Wadt, W. R. *J. Chem. Phys.* **1985**, *82,* 270. (c) Wadt, W. R.; Hay, P. J. *J. Chem. Phys.* **1985**, *82,* 284. (d) Hay, P. J.; Wadt, W. R. *J. Chem. Phys.* **1985**, *82,* 299.
(26) Fukui, K. *Acc. Chem. Res.* **1981**, *14*, 363.
(27) (a) Tomasi, J.; Persico, M. *Chem. Rev.* **1994**, *94*, 2027. (b) Tomasi, J.; Cammi, R. *J. Comput. Chem.* **1996**, *16*, 1449.
(28) Frisch, M. J., et al. *Gaussian 03*, Revision C.02; Gaussian, Inc., Wallingford, CT, 2004.

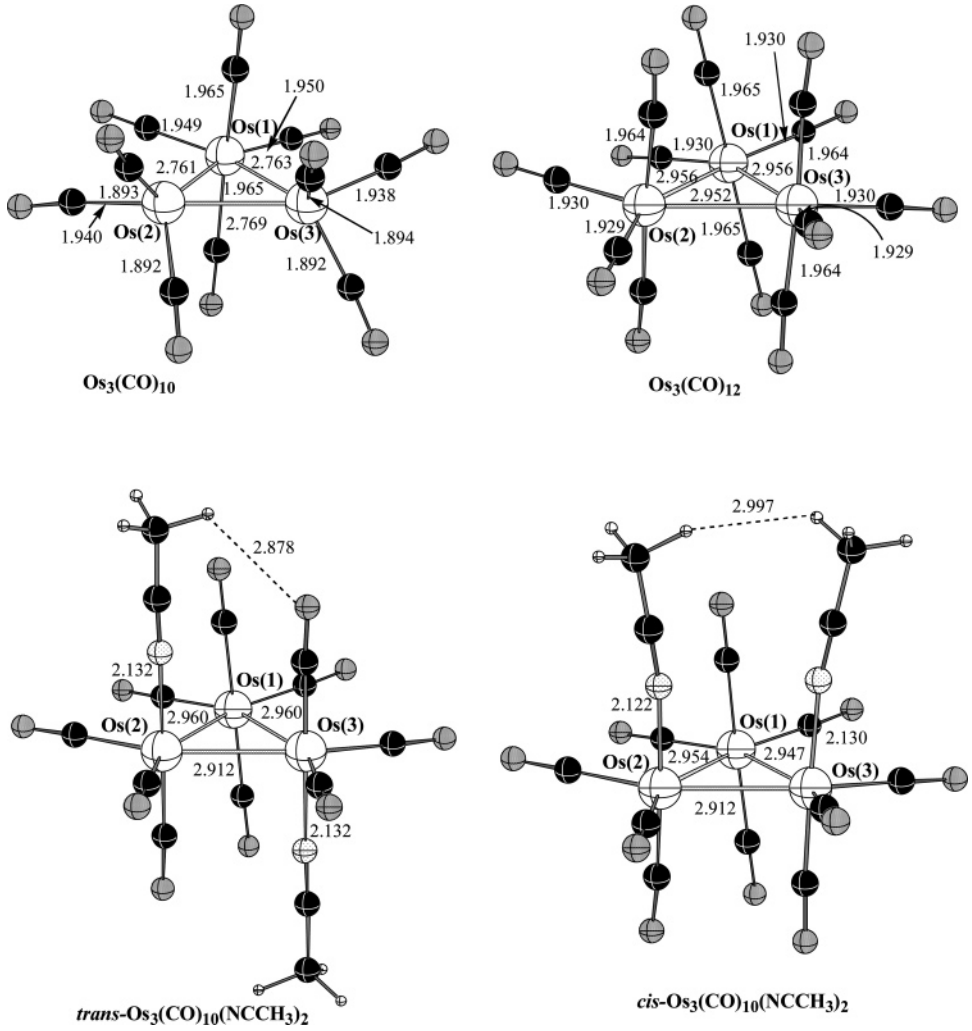

Figure 1. Optimized structures (distances are given in Å) for the reference compounds $Os_3(CO)_{10}$, $Os_3(CO)_{12}$, and the cis and trans isomers of $Os_3(CO)_{10}(CH_3CN)_2$.

quinoline (**3**), indoline (**4**), 1,2,3,4-tetrahydroquinoline (**5**)) and the triosmium cluster $Os_3(CO)_{10}$, where the nitrogen atom has coordinated to one osmium with a donor bond and the C−H bond β to the nitrogen has undergone an oxidative addition to form a bridging hydride and a covalent bond to a second osmium atom (eq 1).

$$Os_3(CO)_{10} + L \rightarrow Os_3(CO)_{10}(\mu_2\text{-}\eta^2\text{-}(L{-}H))(\mu\text{-}H) \quad (1)$$

$$L = \text{benzoheterocycle}$$

Therefore, let us start our discussions of these two components of the complexes **1**−**5**.

Prereaction Complexes: $Os_3(CO)_{10}$, $Os_3(CO)_{11}$, $Os_3(CO)_{12}$, $Os_3(CO)_{10}(CH_3CN)$, and $Os_3(CO)_{10}(CH_3CN)_2$. The hypothetical cluster $Os_3(CO)_{10}$ can be considered as a precursor of the stable complexes $Os_3(CO)_{12}$ and $Os_3(CO)_{10}(CH_3CN)_2$ (eq 2).

$$Os_3(CO)_{10} + 2L \rightarrow Os_3(CO)_{10}L_2 \quad (2)$$

$$L = CO, CH_3CN$$

Interestingly, this 44e$^-$system has been proposed as an intermediate in the reactions of $Os_3(CO)_{10}(\mu\text{-}H)_2$ with alkynes at ambient temperatures,[4,29,30] while its structural parameters have never been reported. In this paper we have fully optimized the geometries of all three complexes as well as the intermediates $Os_3(CO)_{11}$ and $Os_3(CO)_{10}(CH_3CN)$. The optimized structure of $Os_3(CO)_{10}$ and the calculated geometrical parameters of $Os_3(CO)_{12}$ and $Os_3(CO)_{10}(CH_3CN)_2$ are shown in Figure 1. As can be seen from this figure, the disposition of the carbonyl groups in $Os_3(CO)_{10}$ resembles that in the previously reported $Os_3(CO)_{10}(\mu\text{-}H)_2$.[31] The metal−metal bonds are all essentially equal at 2.76 Å and are somewhat shorter than in the calculated structure of $Os_3(CO)_{12}$ (2.96 Å). The Os−Os bonds in the calculated structure for $Os_3(CO)_{12}$ are somewhat longer than those reported in the solid state (2.88 Å),[32] and the $Os(CO)_4$ groups in all the structures exhibit a slight torsion angle not observed in the solid-state structures.[31−33] The Os−CO and C−O bond lengths are both in good agreement with the averages reported for the solid-state structures.[31−33] The calculated gas-phase structure of *trans*-$Os_3(CO)_{10}(CH_3CN)_2$ is in good agreement with the solid-state structure, with the calculated Os−N and nitrile

(29) Keister, J. B.; Shapely, J. R. *J. Am. Chem. Soc.* **1976**, *98*, 1056.
(30) Rosenberg, E.; Anslyn, E.; Aime, S.; Milone, L.; Gobetto, R.; Osella, D. *Gazz. Chim. Ital.* **1988**, *118*, 299.
(31) Churchill, M. R.; Hollander, F. J.; Hutchinson, J. P. *Inorg. Chem.* **1977**, *16*, 2697.
(32) Corey, E. R.; Dahl, L. F. *Inorg. Chem.* **1962**, *1*, 521.
(33) Dawson, P. A. Q.; Johnson, B. F. G.: Lewis, J.; Puga, J.; Raithby, P. R.; Rosales, M. J. *J. Chem. Soc., Dalton Trans.* **1982**, 233.

Table 1. Calculated Binding Energies (in kcal/mol) of the Ligand L to $Os_3(CO)_{10}$ According to the Equations $Os_3(CO)_{10} + 2L \rightarrow Os_3(CO)_{10}L_2$ and $Os_3(CO)_{10} + L \rightarrow Os_3(CO)_{10}L$ (L = CO, CH_3CN) and $Os_3(CO)_{10} + L \rightarrow Os_3(CO)_{10}(\mu_2\text{-}\eta^2\text{-(L-H)})(\mu\text{-H})$ (L = Benzoheterocycle)

L or 2L	compd	ΔG	ΔH
CO		−26.67	−38.58
2CO		−47.30	−72.00
CH_3CN		−10.89	−23.71
$2CH_3CN$ (trans)		−18.66	−43.07
$2CH_3CN$ (cis)		−10.09	−36.22
benzoxazole	**1**	−17.84	−36.00
benzothiazole	**2**	−15.57	−33.74
quinoline	**3**	−15.12	−33.29
indoline	**4**	−10.68 (−9.02)[a]	−29.11 (−27.47)[a]
1,2,3,4-tetrahydro-quinoline	**5**	−3.31 (−0.02)[a,b]	−21.61 (−18.88)[a,b]

[a] These complexes exist as syn and anti isomers; see Figure 2. [b] Compound **5** has not been observed experimentally.

C−N bonds being 2.13 and 1.15 Å, vs 2.13(1) and 1.12 Å in the solid state.[33] The metal−metal bonds are, however, slightly longer for the calculated structure, averaging 2.94 vs 2.86(2) Å in the solid state for $Os_3(CO)_{12}$.[33]

The binding energies calculated according to eqs 1 and 2 are given in Table 1. As expected, the binding energy (here and throughout this paper we will report ΔH and ΔG values (in parentheses), and we will mainly discuss the ΔH values, unless otherwise explicitly stated) for L = CO is much higher than for L = CH_3CN. The calculated gas-phase bond dissociation energy for CO from $Os_3(CO)_{12}$ of 33.4 (20.6) kcal/mol (the binding energy for one CO to $Os_3(CO)_{11}$; Table 1) is in excellent agreement with the enthalpy of activation reported for CO dissociation from $Os_3(CO)_{12}$ in benzene of 35 kcal/mol.[34] The calculated bond dissociation energy of acetonitrile from $Os_3(CO)_{10}(CH_3CN)_2$ of 19.4 (7.8) kcal/mol (the binding energy for one CH_3CN to $Os_3(CO)_{10}(CH_3CN)$; Table 1) is in excellent agreement with the ligand independent enthalpy of activation of 18.9 kcal/mol for one acetonitrile reported for phosphine substitution of $Os_3(CO)_{10}(CH_3CN)_2$ in xylene.[35] Overall, these results lend support to the idea that the other calculated gas-phase energies discussed herein are reliable and can be safely extended to the solution phase for nonpolar solvents.

As expected, the complex $Os_3(CO)_{10}(CH_3CN)_2$ can exist as trans and cis isomers (Table 1 and Figure 1). In the gas phase, *cis*-$Os_3(CO)_{10}(CH_3CN)_2$ is calculated to be less stable than *trans*-$Os_3(CO)_{10}(CH_3CN)_2$ by 6.9 (8.6) kcal/mol, which is clearly due to the added steric crowding resulting from the eclipsing interaction of the acetonitrile ligands in the cis isomer (Figure 1). When corrected for the dielectric of the solvent dichloromethane, in which the reactions for making complexes **1**−**5** were performed, the cis isomer is slightly more stabilized, being 4.0 (5.7) kcal/mol less stable than the trans isomer. Using this difference in ΔG value of 2.9 kcal/mol, an equilibrium constant for *trans*-/*cis*-$Os_3(CO)_{10}(CH_3CN)_2$ is calculated to be 1.4×10^2. These results are reasonable, in light of the previously reported

Table 2. Calculated Reaction Energies (in kcal/mol) for the Reaction *cis*-$Os_3(CO)_{10}(CH_3CN)_2 + L \rightarrow Os_3(CO)_{10}(\mu_2\text{-}\eta^2\text{-(L-H)})(\mu\text{-H}) + 2CH_3CN$ (L = Benzoheterocycle)

compd	ΔG	ΔH
1	−7.75	+0.45
2	−5.48	+8.12
3	−5.04	+3.16
4	−1.98 (−0.32)[a]	+5.47 (+7.11)[a]
5	+6.77 (7.86)[a,b]	+14.61 (15.31)[a,b]

[a] There are syn and anti isomers of **4** and **5**; see Figure 2. [b] Compound **5** has not been observed experimentally.

VT ^{13}C NMR ligand dynamics studies of $Os_3(CO)_{10}(CH_3CN)_2$ in dichloromethane, which show that only the trans isomer is detected in solution.[36] The barrier to the trans to cis interconversion is masked by the carbonyl exchange processes, which occur with barriers of 8−12 kcal/mol, and by the fact that the cis isomer is not detected by NMR.[36] Exchange between free and coordinated acetonitrile was shown to be slow on the NMR time scale—up to 340 K.[36] It is possible that this isomerization is dissociative in nature, but the calculated dissociation energy of 19.4 kcal/mol seems rather high, in light of the fact that related processes in metal carbonyl and isocyanide triosmium clusters take place in the range of 10−15 kcal/mol by intramolecular pathways. It is more likely that the trans/cis isomerization occurs by an intramolecular process with a barrier similar to that for the carbonyl exchange processes but is hidden in the reported ^{13}C NMR spectra.[36] The trans/cis isomerization most likely takes place by two sequential tripodal motions (i.e. axial to radial and radial to axial, involving simultaneous motion of two carbonyl groups and an acetonitrile ligand), a mechanism that has been well documented experimentally for carbonyl groups in trimetallic clusters.[37,38]

Geometrical Structure and Stability of Complexes 1−5. As seen in Table 1, the calculated binding energies of the benzoheterocycles (L) to $Os_3(CO)_{10}$ are significantly smaller than the bond dissociation energy of the two acetonitrile molecules which they replace (−21 to −36 versus −43.1 kcal/mol) from *trans*-$Os_3(CO)_{10}(CH_3CN)_2$, which seems to contradict the description of $Os_3(CO)_{10}(CH_3CN)_2$ as a "lightly stabilized" cluster, in light of the thermal stability of **1**−**5**.[4] Therefore, it is more likely that the complexes **1**−**5** are formed via the higher energy *cis*-$Os_3(CO)_{10}(CH_3CN)_2$, either before or after the initial displacement of one acetonitrile by the heterocycle. That the cis isomer of $Os_3(CO)_{10}(CH_3CN)_2$ is the reactive species in the formation of **1**−**5** is consistent with the rather slow reaction rates observed, owing to its low population.[6,7] On the other hand, the cis isomer may not be necessary if replacement occurs through $Os_3(CO)_{10}(CH_3CN)$ or an associative transition state, but these pathways would require significant reorganization of the carbonyl groups to arrive at the final cisoid configuration of complexes **1**−**5**. As seen in Table 2, where we present the calculated energies of the reaction of *cis*-$Os_3(CO)_{10}(CH_3CN)_2$

(34) Poë, A. J.; Sekhar, V. C. *Inorg. Chem.* **1985**, *24*, 4376.
(35) Dahlinger, K.: Poë, A. J.; Sayal, P. K.; Sekhar, V. C. *J. Chem. Soc., Dalton Trans.* **1986**, 2145.
(36) Aime, S.; Dastrù, W.; Gobetto, R.; Krause, J.; Violano, L. *Inorg. Chim. Acta* **1995**, *235*, 357.
(37) Rosenberg, E.; Day, M.; Espitia, D.; Hardcastle, K. I.; Kabir, S. E.; McPhillips, T.; Gobetto, R.; Milone, L.; Osella, D. *Organometallics* **1993**, *12*, 2390.
(38) Rosenberg, E.; Barner-Thorsen, C.; Milone, L.; Aime, S. *Inorg. Chem.* **1985**, *24*, 231.

with benzoheterocycles (L), using *cis*-$Os_3(CO)_{10}(CH_3CN)_2$ as a prereaction complex results in slightly negative ΔG_{rxn} values and slightly positive (not stable to the dissociation limit) ΔH_{rxn} values for all compounds except for **5** (vide infra) and suggests that the driving force for the formation of **1**−**4** is entropic, as expected from the particle balance shown in eq 3.

$$cis\text{-}Os_3(CO)_{10}(CH_3CN)_2 + L \rightarrow Os_3(CO)_{10}(\mu_2\text{-}\eta^2\text{-}(L-H))(\mu\text{-}H) + 2CH_3CN \quad (3)$$

The formation of **1**−**4** and **5** (vide infra) takes place at 298 K, and although kinetic studies have not been done, the reactions are slow relative to phosphine substitution.[6,7,35] Given the relatively low thermodynamic driving force for the formation of these complexes from *cis*-$Os_3(CO)_{10}(CH_3CN)_2$ (Table 2) and the smaller cone angle of the benzoheterocycles relative to that of PPh_3, the reactions of benzoheterocycles (L) with $Os_3(CO)_{10}(CH_3CN)_2$ at 298 K are expected to have an associative component. Therefore, a likely reaction pathway for formation of **1**−**4** from *cis*-$Os_3(CO)_{10}(CH_3CN)_2$ and the benzoheterocycles could be the heterocycle-induced dissociation of acetonitrile by attack at the metal or nucleophilic attack at coordinated acetonitrile, followed by slow dissociation of the second acetonitrile and C−H or N−H oxidative addition, perhaps induced by agostic C−H or N−H interactions (vide infra).[6] This prediction is further supported by the facts that (a) the complexes $Os_3(CO)_{10}(\mu_2\text{-}H)[\mu_2\text{-}NC(CH_3)(NR_2)]$, whose structures are the result of nucleophilic attack on coordinated acetonitrile, are isolated from the reactions of *cis*-$Os_3(CO)_{10}(CH_3CN)_2$ with cyclic amines (eq 4)[6] and (b) kinetic studies suggest that substitution of the first acetonitrile labilizes the dissociation of the second acetonitrile.[35]

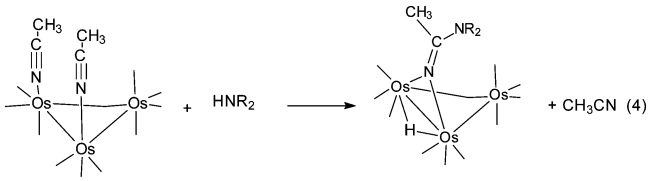

As seen in Table 1, the calculated binding energies for the aromatic ligands in **1**−**3** are significantly higher than in **4** and **5**. This trend might be explained in terms of the greater basicity of the pyridine type nitrogen atoms relative to the aniline type nitrogen atoms in **4** and **5**.

As can be expected from the geometrical structures of the complexes **4** and **5**, they may exist as two isomers which differ in the relative disposition of the N−H bond with respect to the triangular face of the cluster, syn or anti. These two isomers were also proposed from ^1H NMR studies and were observed experimentally for compound **4**, where the ratio of the two isomers was found to be 2.5:1 ($\Delta G = -0.54$ kcal/mol).[6] However, we did not know whether the syn or anti isomer was more stable, because the stereochemical disposition of the N−H was not known in the absence of solid-state structural data, as **4** is unstable with respect to conversion to **4′** (vide infra).[19] The optimized structures of *syn*- and *anti*-**5** as well as the bond lengths for **4** (bond lengths for **5** are given in parentheses) are shown in Figure 2. For **4**, the isomer with the N−H bond syn to the triangular face of the cluster is 1.6 (1.7) kcal/mol ($K_{eq} = 17.8$) more stable than the anti isomer. When it is corrected for the dielectric of the solvent, dichloromethane, the energy gap between the syn and anti isomers is slightly reduced to 1.1 (1.1) kcal/mol ($K_{eq} = 6.5$). For the hypothetical complex **5** the syn isomer lies 2.7 (3.3) kcal/mol lower in energy than the anti isomer.

The slightly greater stability of the syn isomer for both **4** and **5** is at least in part due to the existence of the weak hydrogen-bonding interaction between the NH fragment and the axial CO on the unbridged Os atom; the calculated N−H···OC distance to the oxygen atom of that carbonyl group is 2.5 Å (Figure 2). Such N−H···OC distances have been invoked as evidence of weak H-bonding between amine hydrogen atoms and carbonyl oxygen atoms in the solid state.[39] Interestingly, the N−H···CO distance is even shorter at 2.3 Å, suggesting that, in this rare intramolecular example of carbonyl group hydrogen bonding, the primary interaction may be with the polarized π electrons of the CO group rather than with the oxygen lone pair. This is reminiscent of the π-η^2 interactions of carbonyl groups observed in polynuclear carbonyl complexes.[40] The distances from the N−H hydrogen to the other CO ligands in both the syn and anti isomers are all greater than 2.6 Å.

Mechanisms of Decarbonylation and N−H Bond Activation for Compounds 1−5. The decarbonylation of compounds **1**−**3** to yield **1′**−**3′** is a distinctly different process from the conversion of **4** to **4′** and of **5** to **5′**. The decarbonylation of compounds **1**−**3** to yield **1′**−**3′** involves (a) CO dissociation, (b) Os−C bond formation, and (c) the apparent H migration from one edge of the osmium triangle to another. Meanwhile, the conversion of **4** to **4′** and of **5** to **5′** most likely starts with the N−H bond oxidative addition to the cluster, forming a dihydride complex, and then involves all the processes listed above.

As mentioned above, the starting point of **1**−**3** to **1′**−**3′** conversion should be the decarbonylations of **1**−**3**. Experimental studies show that compounds **1**−**3** lose CO only at high temperatures (>100 °C) or by photochemical means to give the highly reactive coordinately unsaturated species **1′**−**3′**.[7] As shown in Table 3, the DFT calculations for the decarbonylation of **1**−**3** show positive free energies and enthalpies of reaction, as expected for the formation of the corresponding 46e coordinately unsaturated clusters **1′**−**3′**. The calculated energetics for the decarbonylations of **1**−**3** also shed light on the experimental trends observed for the carbonylations of **1′**−**3′**, which lead to cleavage of the benzoheterocycle and formation of $Os_3(CO)_{12}$ (Scheme 1).[39,40] Compound **1′** undergoes cleavage of the benzoheterocycle much more slowly (25% complete after 240 h at 70 °C) than compound **3′** (100% complete after 24 h), while conversion of the nonacarbonyl to the corresponding decacarbonyl (**1′** to **1** and **3′** to **3**) is relatively fast in both cases.[41,42]

(39) Braga, D.; Grepioni, F. *Acc. Chem. Res.* **1997**, *30*, 81.
(40) Hermann, W. A.; Ziegler, M. L.; Weidenhammer, K.; Biersack, H.; *Angew. Chem., Int. Ed. 18*, 961.
(41) Rokhsana, D. Doctoral Thesis, University of Montana, Missoula, MT, 2005.
(42) Rosenberg, E.; Abedin, J.; Rokhsana, D.; Viale, A.; Dastrù, W.; Gobetto, R.; Milone, L.; Hardcastle, K. I. *Inorg. Chim. Acta* **2002**, *334C*, 343.

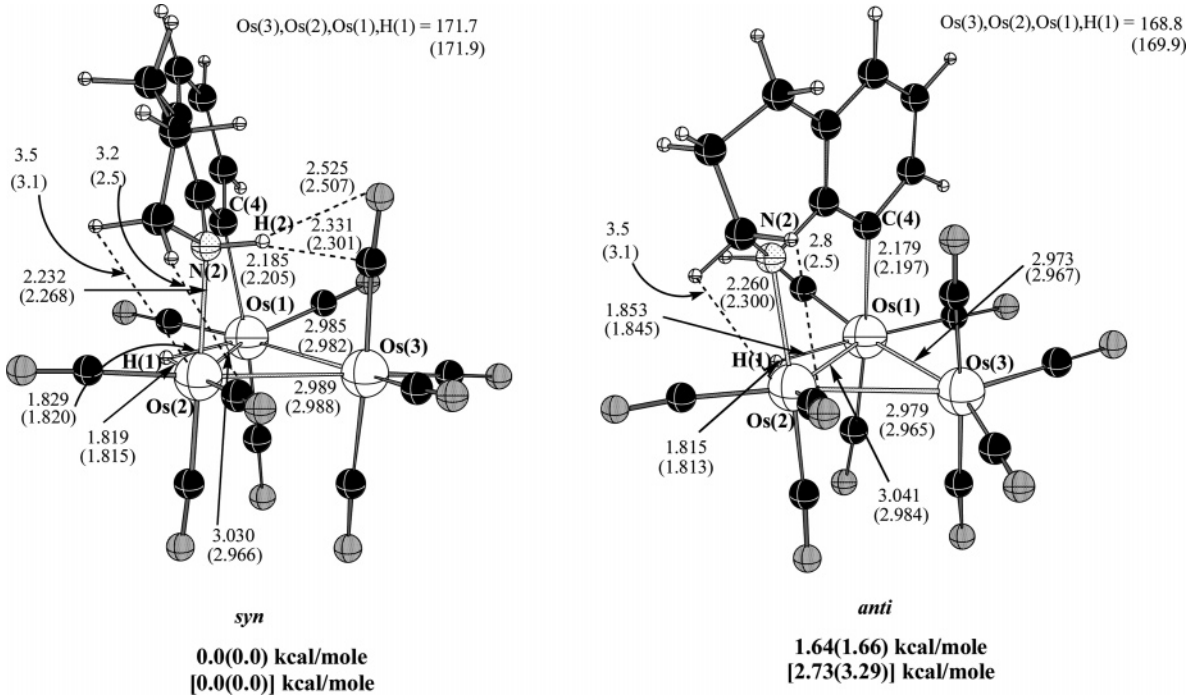

Figure 2. Optimized structures (distances are given in Å) for the syn and anti isomers of **4** and **5**, showing important bond distances (distances for **5** are given in parentheses, while its relative energies are given in brackets).

Table 3. Decarbonylation Energies of Compounds 1−5 (kcal/mol)

compd	ΔG	ΔH
1	+11.28	+23.08
2	+8.67	+20.20
3	+5.36	+17.00
4	−0.41 (−2.07)[a]	+11.15 (+9.61)[a]
5	−2.29 (−5.56)[a,b]	+8.19 (+5.45)[a,b]

[a] The value in parentheses is for the less thermodynamically stable isomer (N−H anti to the cluster). [b] Compound **5** has not been observed experimentally.

Even though the first step, addition of CO, appears to be fast in both cases, the difference in the observed overall rate of cleavage could be due to (1) a difference in the energy of the transition state for carbonylation, (2) the difference in the relative stabilities of the two decacarbonyl species **1** and **3**, and (3) a difference in the barrier to benzoheterocycle dissociation in the second step. It seemed reasonable to examine this question by at least modeling the reverse of the first step, decarbonylation, as this would also yield fundamental information on how sensitive the decarbonylation process is to the nature of the heterocycle.

We have studied the transition states for the decarbonylation of **1** and **3**. The transition state for the decarbonylation of **2** is expected to be very similar to that for **1** and was not studied. The located transition states for the decarbonylation of **1** and **3** are shown in Figure 3. As seen from this figure, they involve Os−C stretching and Os−C−O bending of the axial carbonyls on the same side of the cluster triangle as the ring, a twisting around the Os−N axis, and formation of the Os−C(4) bond. We did not examine the transition state for the dissociation of the axial CO trans to the heterocycle on the $Os(CO)_4$ group, because even at room temperature the carbonyl site exchange is rapid with respect to CO dissociation and therefore would have a redundant transition state.[36−40] The calculated imaginary frequencies associated with these transition states are small, 93*i* and 115*i* cm^{-1} for **1** and **3**, respectively, reflecting the endothermicity of the reaction.

The activation energy for this process is 33.8 (31.1) kcal/mol ((30.4) kcal/mol at 100 °C) for **1** and 33.1 (30.8) kcal/mol ((30.2) kcal/mol at 100 °C) for **3**. The ΔH values associated with these decarbonylations are very similar to the ΔH values of activation for CO dissociation from $Os_3(CO)_{12}$, reported above, and suggest that the rates of CO dissociation are insensitive to the nature of the ligand on the trimetallic core.

A pseudo-IRC calculation was performed by slightly elongating the Os−CO bond distance in the transiton state and optimizing the geometry of the resulting structure, confirming that these transition states connect **1** with **1a′** and **3** with **3a′**, respectively. The resulting structures **1a′** and **3a′** (Figure 3) are hydride positional isomers of **1′** and **3′** and lie (2.5) and (4.5) kcal/mol above the experimentally observed **1′** and **3′**. These structures can easily (with a small barrier) rearrange to **1′** and **3′**. It is noteworthy that, in our NMR studies of the carbonylation reaction conversion of **3′** to **3** using ^{13}CO, we found that this process involves hydride edge to edge migration, or edge to edge migration of the heterocycle pivoting on the Os−C and Os−N bonds at ambient temperatures.[7] It does not seem fruitful, at this time, to try to model this multiple pathway process. Rather, we are currently investigating the transition states for hydride migrations in complexes where only hydride migration is taking place and where more quantitative experimental data are available.

The conversion of **4** to **4′** and of **5** to **5′** likely starts with the N−H bond oxidative addition to the cluster forming a dihydride complex and involves all the processes listed above for **1**−**3** to **1′**−**3′** conversion. Although compound **5** is not observed experimentally, in the calculation it converts to **5′** at room temperature, and both **5** and **5′** are real minima on the potential

Scheme 1. Relative Rates of Cleavage of 1 and 3 from the Triosmium Cluster

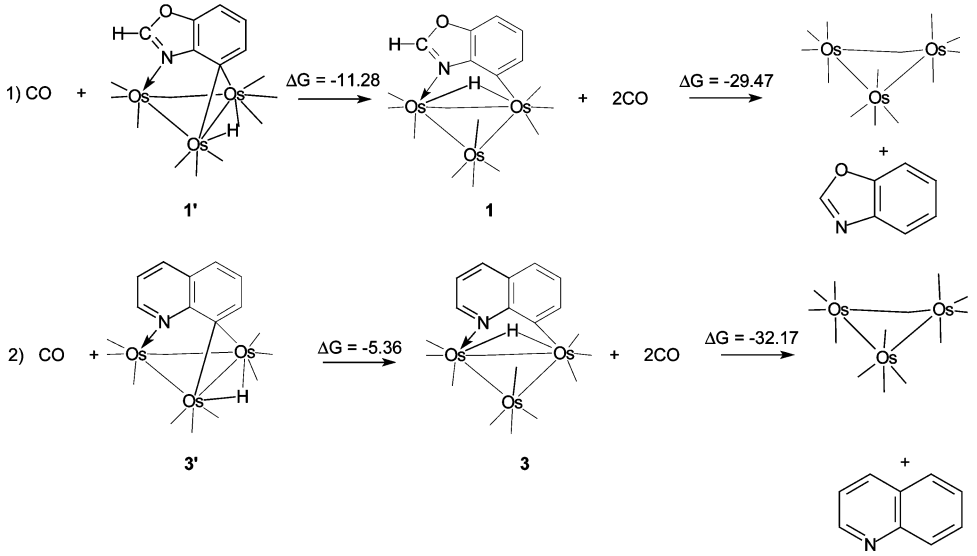

energy surface. Both compounds **4** and **4′** are experimentally observed, but compound **4** converts to **4′** at slightly higher temperatures, 60 °C, with a first-order rate constant of $(1.8 \pm 0.2) \times 10^{-5}$ s^{-1} ($\Delta G^{\dagger} = 30.2$ kcal/mol at 60 °C). Furthermore, both isomers (syn and anti) of **4** appear to convert to **4′** at the same rate.[6]

On the basis of the calculated structures, the reason **5** converts to **5′** at lower temperatures (i.e. with a lower barrier) than for **4** to **4′** is believed to be steric in origin (Figure 2). Indeed, the presence of an additional methylene group in **5** results in additional steric crowding between the methylene, adjacent to the nitrogen atom, and the Os atom bound to nitrogen, as well as the radial CO ligand trans to the hydride ligand. The distance from one of the methylene hydrogen atoms to the nitrogen-bound Os atom is 3.1 Å (bond distances for **5** are given in parentheses in Figure 2), and the distance from the other methylene hydrogen to the radial CO trans to the hydride ligand is 2.5 Å in the syn isomer. The corresponding distances in **4** are 3.5 and 3.2 Å, respectively. The situation is almost the same for the anti isomer. The Os−N bonds in **5** are slightly longer (2.26 and 2.30 Å) than in **4** (2.23 and 2.26 Å) in the syn and anti isomers, respectively. This steric crowding may account for the lower binding energy and the positive free energy of reaction for formation of **5** and may be the underlying reason **5** is not observed experimentally, assuming that the transition states for the conversion of **5** to **5′** and **4** to **4′** are similar in energy (Table 2). To address this point, we have attempted to model the transition state for these transformations. We discuss it only for compound **4**, since this compound is observed experimentally while **5** is not and we therefore have no way of calibrating the relevance of the results.

The more complex N−H activation/decarbonylation process involved in the conversion of **4** to **4′** can be viewed as a two-step process, although in reality it may be a concerted process, where anchiomeric assistance

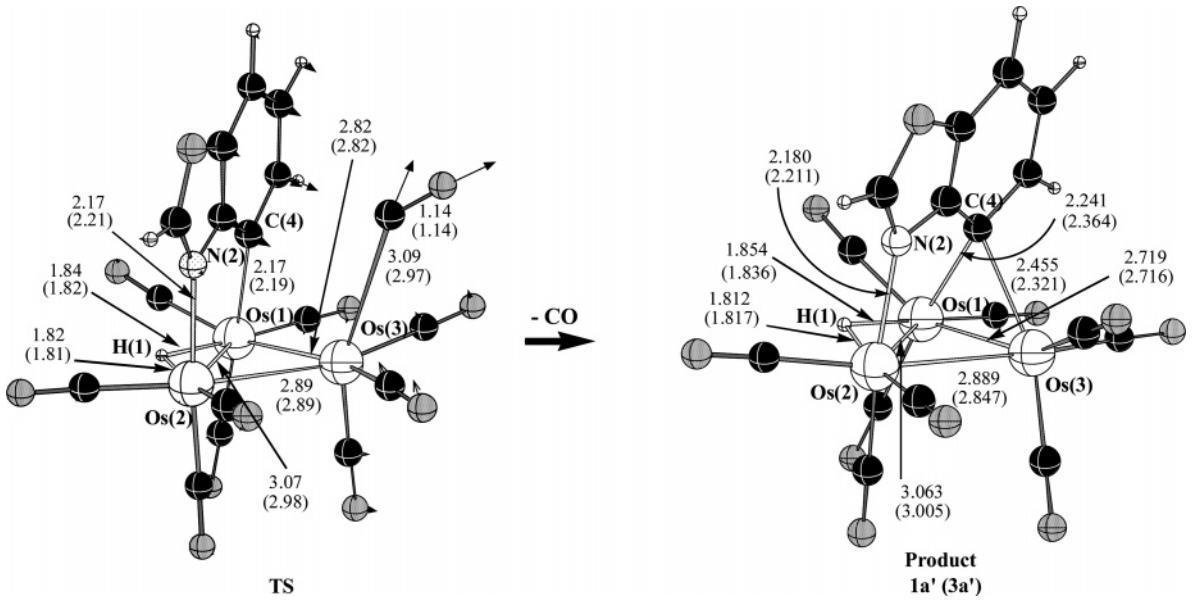

Figure 3. Transition states for the decarbonylation of **1** and **3** showing important bond distances (distances for **3** are given in parentheses), the normal mode vectors associated with the reaction coordinate (arrows for **1** only), and the product obtained from pseudo-IRC calculations (hydride positional isomers of **1′** and **3′**). Distances are given in Å.

Scheme 2. Schematic Representation of the Potential Energy Surface for the Conversion of 4 to 4′[a]

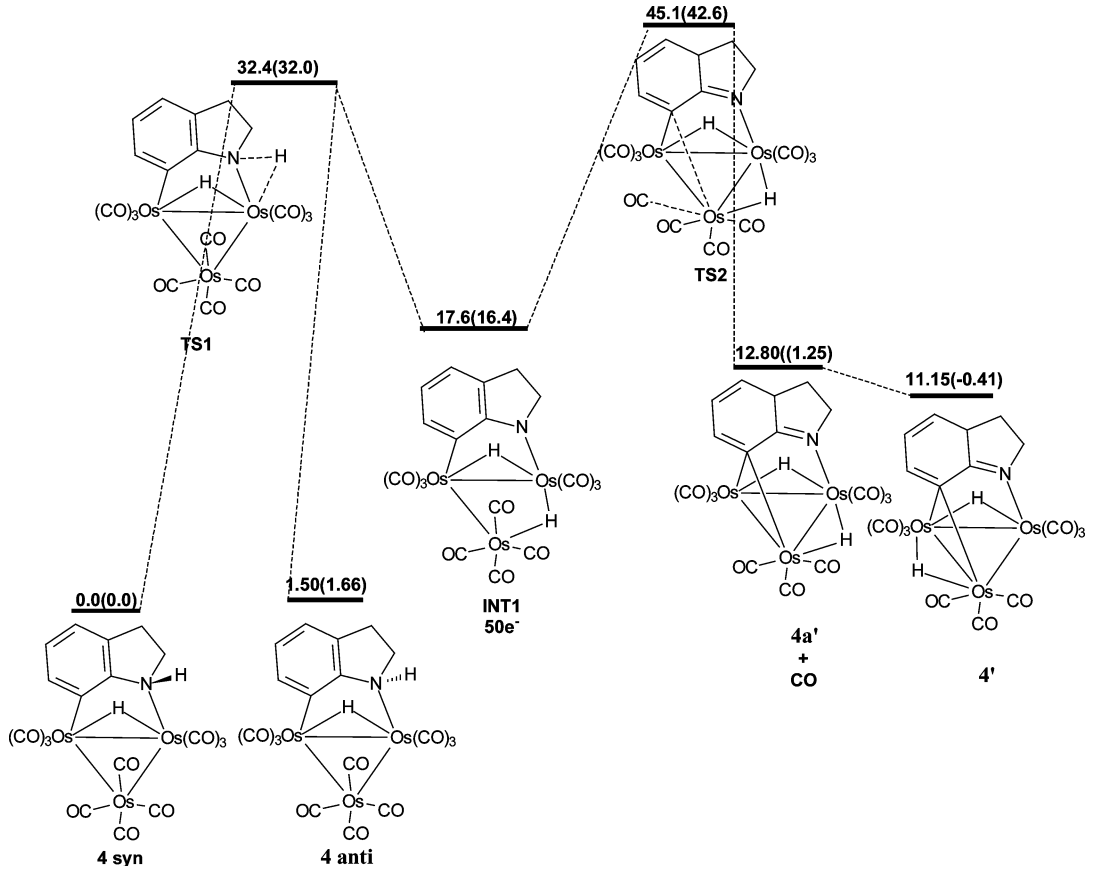

[a] ΔH values (and ΔG values in parentheses) are given in units of kcal/mol.

by nitrogen induces decarbonylation at an adjacent osmium as has been noted for decarbonylation in pyridinyl triosmium clusters.[43] Even if the process is concerted, treating it as a two-step process will reveal which of the two steps is slower and whether decarbonylation from the expected 50e dihydride intermediate is a higher or lower energy process than CO dissociation from the 48e clusters **1**−**3.** The results of these calculations are summarized in Scheme 2. The optimized transition state structure for the two-step process of N−H oxidative addition **TS1** and the 50e intermediate **Int1** are shown in Figure 4. The transition state for the second step **TS2** is also shown in Figure 4.

The slower step in the reaction is the activation of the N−H bond, and the calculated free energy of activation for this step, $\Delta G^{\ddagger} = 32.0$ kcal/mol (at 60 °C), is in reasonable agreement with the experimental value of $\Delta G^{\ddagger} = 28.2$ kcal/mol at the same temperature. This step involves increasing involvement of metal electron density in the elongated N−H bond in **TS1**, as evidenced by the decreased positive NPA charge on H from 0.431e in **4** to 0.075e in **TS1**, while the charge on N remains essentially constant, being −0.667e in **4** and −0.659e in **TS1**. The intermediate **Int1** shows the expected highly elongated Os−Os distance along the edge bridged by the newly formed hydride. This distance of 3.44 Å indicates no bonding between Os(2) and Os(3). The Os−N is now an amide bond, and the nitrogen has a lone pair. This is apparent from the shortening of the Os−N bond from 2.17 Å in **4** to 2.06 Å in **Int1**. Taken together, this information gives a useful description of the process of N−H activation at a polymetallic site. The transition state found for this particular case involves hydrogen transfer to the Os(2)−Os(3) edge rather than to one metal atom (i.e. Os(2)). The bond lengths to each metal are fairly similar (Os(2)−H(2) = 1.97 Å, Os(3)−H(2) = 1.92 Å) and are not too much longer than the typical bridging hydride bond length of 1.81−1.84 Å in this type of cluster.[6,7] Taken together with the highly elongated N−H bond of 1.57 Å (1.02 Å in the reactant **4**) and the decreased positive charge on H, **TS1** can be described as a late transition state. Pseudo-IRC calculations were performed to verify **TS1**. A transition state similar to **TS1** could also be approached from the less thermodynamically stable anti isomer but would require prior or successive migration of the bridging hydride in **4**, a process which is definitely energetically accessible at ambient temperatures on the basis of previous studies with related systems (Scheme 2 shows only the energetics for the syn isomer).[6,7] The geometry and therefore the energy of this transition state would be slightly different from those of **TS1**. The energy required to reach **TS2** from **Int1**, 27.5 (26.2) kcal/mol, is significantly lower than the ∼33 (∼31) kcal/mol calculated for **1**-**3**; this is in agreement with experiment, since **4** undergoes conversion to **4′** at 60 °C at about the same rate as **1**−**3** do at 100 °C. The overall reaction rate, however, should be determined by the transition state with the highest energy, i.e., the CO dissociation step at 45.1 (42.6) kcal/mol above the reactant **4**, and this is

(43) Deeming, A. J.; Smith, M. B. *J. Chem. Soc., Chem Commun.* **1993**, 844.

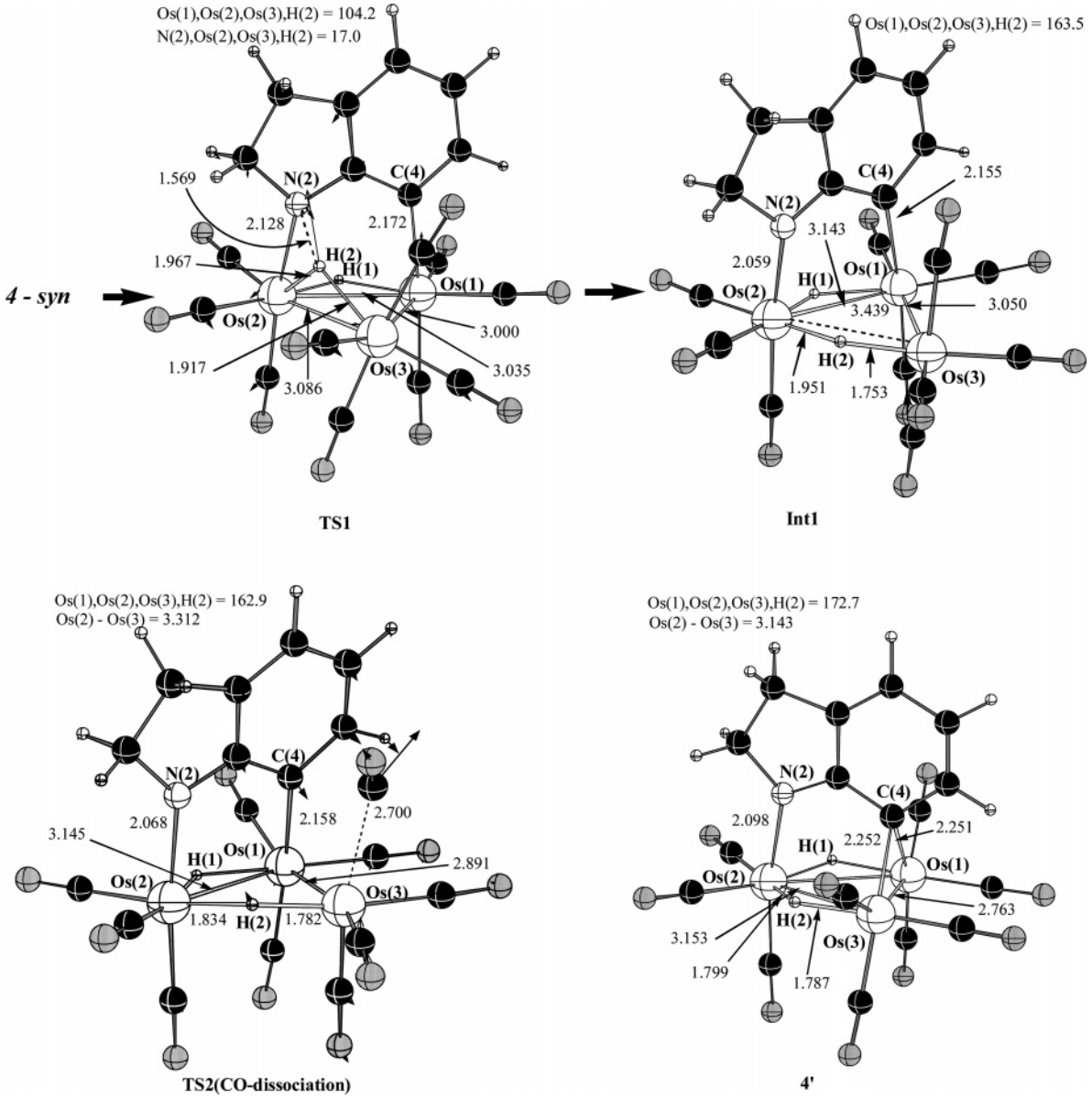

Figure 4. Transition states **TS1** and **TS2** for the N−H bond activation in the conversion of **4** to **4′**, showing relevant bond lengths (in Å) and normal mode vectors, and the optimized geometries (distances given in Å) for the 50e intermediate **Int1** and the kinetic product **4a′** (hydride positional isomer of **4′**) obtained from **TS2**.

apparently not the case here. This suggests that the CO dissociation is significantly coupled with **TS1**. We attempted to find a concerted transition state for the conversion of **4** to **4′**, but these attempts led to structures with multiple imaginary frequencies. In a molecule such as **4** (and **5**) there are a myriad of pathways by which this could occur, and attempts to model this will be the subject of a future study. On the other hand, the present calculation does not necessarily rule out the two-step pathway but may only overestimate the barrier. As one might expect, the calculations do point out that CO dissociation from a higher energy 50e cluster such as **Int1** should be a faster process than that from related 48e systems such as **1**−**3**.

Analysis of the Electronic Structure and Bonding in the Complexes 1, 3, and 4 and Their Nonacarbonyl Analogues. To analyze the electronic structure and the bonding nature in the isostructural molecules **1**, **3**, and **4**, we have performed natural population analyses (NPA) on the optimized structures of these species. These three compounds were chosen because they represent three distinct structural types, while **2** and **5** are direct analogues of **1** and **4**. To simplify our analyses, we have divided NPA charges into the four different parts of the molecule: organic ligand, all carbonyl ligands, metal core, and hydride ligand (Q_{L-H}, Q_{CO}, Q_{Os_3}, and $Q_{\mu-H}$, respectively). The calculated charges of these fragments are shown in Tables 4 and 5. The most obvious trend in the presented data is that over the series the net electron density at the metal (Q_{Os_3}) and the bridging hydride ($Q_{\mu-H}$) remains nearly constant. Thus, the pronounced differences in electron distribution in these systems are between the benzoheterocycle and the carbonyl ligands, with the metal core acting as a conduit for distributing the electronic charge. The carbonyl ligands have a net positive charge, which is consistent with the much higher binding energies found for CO versus the benzoheterocycle (L−H) (Table 1). The greater residual negative charge on the fully aromatic ligands in **1** and **3** relative to indoline

Table 4. Net Electronic Ligand and Metal Core Charges (Q) and CO Charge Separations in the $Os_3(CO)_{10}(\mu_3\text{-}\eta^2\text{-(L-H)})(\mu\text{-H})$ Complexes

					ΔQ_{CO}			
compd	Q_{Os_3}	$Q_{\mu-H}$	Q_{CO}	Q_{L-H}	trans to N	trans to C	Q on N	Q on C
1	−0.33	−0.17	+0.74	−0.24	0.14	0.09	−0.53	−0.28
3	−0.33	−0.14	+0.72	−0.22	0.15	0.09	−0.48	−0.29
4	−0.33	−0.16	+0.66	−0.17	0.15	0.08	−0.67[a]	−0.29

[a] Bound to a hydrogen atom that has natural charge of +0.43e.

Table 5. Net Electronic Ligand and Metal Core Charges (Q) and CO Charge Separations in the Complexes $Os_3(CO)_9(\mu_3\text{-}\eta^2\text{-(L-H)})(\mu\text{-H})$ (1′ and 3′) and $Os_3(CO)_9(\mu_3\text{-}\eta^2\text{-(L-2H)})(\mu\text{-H})_2$ (4′)

					ΔQ_{CO}			
compd	Q_{Os_3}	$Q_{\mu-H}$	Q_{CO}	Q_{L-H} or Q_{L-2H}	trans to N	trans to μ-C	Q on N	Q on C
1′	−0.28	−0.15	+0.58	−0.18	0.09	0.14	−0.52	−0.46
3′	−0.28	−0.15	+0.56	−0.11	0.08	0.14	−0.47	−0.47
4′	−0.27	−0.15	+0.57	−0.15	0.08	0.13	−0.47	−0.47

in **4** is consistent with their expected greater electron affinity and suggests that the π-acceptor character of the ligand is of particular importance in this series of complexes. The magnitude of the residual charge on the benzoheterocycle follows the order of the binding energies **1** > **3** > **4**, but the differences are small, and it would be inappropriate to make a quantitative comparison.

A much more pronounced correlation can be made between the charge on heterocycle atoms bound to the osmium triangle and the degree of charge separation (bond polarization, ΔQ) in the carbonyl ligands (Tables 4 and 5), particularly when comparing **1** to **1′** and **3** to **3′**. The charge on the metal-bound carbon atom (Q on C) of the ligand becomes more negative by 0.18e on going from the decacarbonyl to the nonacarbonyl derivatives. This is paralleled by a 0.05e increase in bond polarization for the carbonyl groups trans to carbon and decrease in the bond polarization for the carbonyl ligand trans to nitrogen, although its charge is unchanged. Carbonyl bond polarization is normally associated with increased σ donation by the ligand trans to the carbonyl and in this case implies a significant change in the type of bonding of the carbon attached to the Os atom. The Os−N bond lengths are essentially the same in all the complexes, and the Os−C bonds increase on going from the two-center to the three-center bonding.[10] The significant changes in trans-CO bond polarization imply an increased σ-donor component in **1′** and **3′** relative to that in **1** and **3** by the carbon atom and a decreased σ component in the Os−N bond, perhaps with compensating increased π component to account for the constancy of the Os−N bond length and charge on N. Significantly, both the charge increase and the increased bond polarization going from a terminal to a bridging carbon in **1** and **3** versus **1′** and **3′** suggest an increase in σ donation to the metal. This is also seen in the electron-precise cluster **4′**, where the charges on the analogous carbon atom are −0.29e and −0.47e in **4** and **4′** and the *trans*-CO bond polarization increases from 0.08e to 0.13e (Tables 4 and 5).

Overall, the picture that emerges from the NPA is that the carbonyl ligands are responsible for most of the net transfer of electron density to the metal core, and there is a "push−pull" relationship between the carbonyl ligands and the heterocycles. This picture is also supported by the NPA of $Os_3(CO)_{12}$, where the charge on the metal core, −0.57e, is much larger than that for the decacarbonyl and nonacarbonyl complexes given in Tables 4 and 5, respectively. The CO bond polarization in $Os_3(CO)_{12}$ ranges from 0.04 to 0.05e, where the CO ligands trans to the Os−Os show a polarization of 0.05e and the axial carbonyls all show 0.04e.

Conclusions

In conclusion, the DFT calculations on this series of organometallic clusters have provided both mechanistic and thermodynamic information that has elucidated several aspects of their reactivity, including: (1) the structural reasons for the relative stability of reactive intermediates where solid-state structures were not available (**4** and **4′** versus **5** and **5′**), (2) the transition states for decarbonylation of **1** and **3**, where the similarity of the enthalpies of CO dissociation to each other and to $Os_3(CO)_{12}$ demonstrates the insensitivity of this process to the ancillary ligands on the cluster, and (3) the descriptions of likely transition states for N−H activation (in **4**) and the decarbonylation of a 50e intermediate.

The conclusions stated above regarding steric control of reaction energetics speak for themselves. On the other hand, the NPA analyses indicate some degree of orbital control of reaction. However, in molecules such as those discussed in this report the existence of many orbitals with very close energy makes an analysis of possible orbital control nearly impossible. We have therefore refrained from such considerations and maintain that the NPA analyses are at least an important component in understanding the bonding in these systems.

Studies are currently underway that will further extend the applications of the DFT approach to the dynamics and reactivity of related systems. The subsequent NPA provides insight into the net donor abilities of various ligands and their σ-donor/π-acceptor characteristics, which could prove useful in making IR and NMR spectral assignments.

In general, the results reported herein have been correlated with the known experimental data for the subject complexes and have been used to clarify the previously reported reactivity trends.

Acknowledgment. Support for this research by the Department of Energy (E.R., Grant No. DE-FG02-01ER45869) and National Science Foundation (K.M. and D.G.M., Grant No. CHE-0209660) is gratefully acknowledged. E.R. wishes to thank the Cherry Emerson Center for Scientific Computation for a Visiting Fellowship Award and for use of its computational resources.

Supporting Information Available: A table giving Cartesian coordinates for all structures reported in this paper and text giving the complete ref 28. This material is available free of charge via the Internet at http://pubs.acs.org.

OM050711B